Unique Crystalline Orientation of Poly[(*R*)-3-hydroxybutyrate]/Cellulose Propionate Blends under Uniaxial Drawing

Jun Wuk Park, Yoshiharu Doi, and Tadahisa Iwata*

Polymer Chemistry Laboratory, RIKEN Institute, 2-1 Hirosawa, Wako-shi, Saitama 351-0198, Japan

Received September 8, 2004; Revised Manuscript Received December 16, 2004

ABSTRACT: Blends of poly[(*R*)-3-hydroxybutyrate] (PHB) and cellulose propionate (CP) with various compositions were prepared by the solvent-casting method, and their uniaxial drawing behavior was studied by means of two-dimensional wide-angle X-ray diffraction (WAXD) and small-angle X-ray scattering (SAXS). Although this system has been reported to be entirely miscible, the DSC results revealed that the glass transition temperatures of the blends were not composition-dependent in the whole composition range. Furthermore, these transitions were quite broad or even double in the blends with high CP content. These features are the result of differing molecular motions attributed to the difference in chemical structure between the two components of the blend. The feasible maximum draw ratio decreased with increasing CP content due to restraint of chain slippage and necking caused by the stiffness and high friction coefficient of the CP component. A remarkable feature during uniaxial drawing was that the manner of crystallization of the PHB component under strain varied from the *c*-axis-oriented to the *a*-axis-oriented crystal growth with increasing CP content. WAXD analysis demonstrated that drawn pure PHB exhibited an ordinary *c*-axis-oriented pattern, indicating that the (110) and (020) main reflections of PHB were concentrated on the equatorial line. On the contrary, when the CP content was 50 wt %, the diffraction texture was transformed to the *a*-axis orientation where the (110) reflection was located near the meridian and the (020) and (002) reflections lay on the equatorial line. In the SAXS patterns of the blends containing 30−50 wt % CP, instead of meridional spots, the equatorial streaks were clearly observed, providing direct evidence for lamellar stacking perpendicular to the stretching direction. Such a change of crystalline orientation was found to be strongly dependent on the draw ratio and annealing temperature in addition to the blend composition. In the present paper, a mechanism based on the intramolecular nucleation and confined crystal growth model was suggested to interpret this uncommon orientation behavior.

Introduction

Bacterial poly[(*R*)-3-hydroxybutyrate] (PHB) and its related microbial polyesters produced from renewable carbon sources by a number of bacteria have attracted much attention in terms of the biodegradability and biocompatibility. However, the high production cost is still a major obstacle to limit their application to biomaterials in the medical field. Furthermore, its brittleness, instability in the molten state, and consequent narrow processing window also prevent wider scale applications. Blending with a second polymeric component is one of the adequate methods to solve this problem, which can supply opportunities not only to impose the desirable property but also to lower cost. In this viewpoint, blends between PHB and cellulose esters (CEs), which are known to be miscible over the entire composition range despite the large difference in chemical structure, have received much attention.[1−7]

Scandola and co-workers studied aspects of the miscibility and crystallization behavior of these blends in detail by means of calorimetric (DSC) and dynamic mechanical (DMTA) measurements.[1−3] According to these reports, when the PHB content was higher than 50−60%, the bacterial polymer could crystallize from a melt-quenched blend. However, if the cellulose esters content exceeded 50%, PHB was impossible to crystallize and fully amorphous blends were obtained. In addition, the glass transition temperature (T_g) exhibited dual dependence on composition. In the range of CE content 50−100%, the T_g was strongly dependent on composition, whereas a much less substantial dependence was observed at higher than 50% PHB content.[2] Nevertheless, these blend systems were found to show typical thermal behaviors of a miscible system such as a depression of the equilibrium melting point and a remarkable decrease in the crystallization rate.[3] While space-filling spherulites were observed at higher than 50 wt % PHB content, the spherulite growth was significantly retarded by blending with CE. In addition, a remarkable reduction in crystallinity by addition of CE could enhance the toughness significantly.[4] The degradation properties have also been reported to be affected by blending with CE. Wang et al.[5] examined the degradability of PHB/cellulose acetate butyrate (CAB) blends under two conditions, in an acidic or alkaline medium and in a natural environment. In the former case, the degradation was accelerated by blending with CAB, whereas the degradation rate in natural water decreased with increasing CAB content due to the steric hindrance of constituents in CAB.

In this work, the blend of PHB with cellulose propionate (CP) was investigated in terms of uniaxial drawing behavior. Recently, our research group has suggested a novel processing method via cold-drawing and/or two-step drawing for obtaining high-performance PHB films[8,9] or fibers[10] having enhanced flexibility as well as high tensile strength. Furthermore, this enhanced physical property could be preserved without deterioration for a long-term storage at room temperature. In the present work, we attempted to apply this cold-drawing procedure to PHB-based blends with CP.

* To whom correspondence should be addressed. E-mail: tiwata@riken.jp. Phone: +81-48-467-9586. Fax: +81-48-462-4667.

10.1021/ma0481611 CCC: $30.25
Published on Web 02/10/2005

Table 1. Drawing Conditions and Maximum Draw Ratios of PHB/CP Blends

PHB/CP system	CP content (wt %)	drawing temp (°C)	max draw ratio (λ)
PHB	0	4	10
9/1	10	4	7
7/3	30	10	7
5/5	50	60	5
3/7	70	120	3
CP	100	175	3

Particularly, during uniaxial drawing with PHB/CP blends, a unique orientation behavior depending on the blend composition and drawing condition was observed, which is considered to be the result of the differing chain motions caused by dissimilarity in the chemical structure of the two components. Such a unique crystal orientation was investigated in detail by means of X-ray analysis and discussed with reference to several models previously suggested for interpreting the appearance of an uncommon orientation.

Experimental Section

Materials. Bacterial PHB ($M_w = 5.9 \times 10^5$, $M_w/M_n = 2.6$) was supplied by Monsanto Co. Ultrahigh molecular weight PHB (UHMW-PHB, $M_w = 5.3 \times 10^6$, $M_w/M_n = 1.7$) was biosynthesized from glucose by recombinant *Escherichia coli* XL-1 blue (pSYL105) bearing *Ralstonia eutropha* H16 PHB biosynthesis *phbCAB* genes by the method reported previously.[11] Two kinds of PHB were reprecipitated using chloroform as a solvent and *n*-hexane as a nonsolvent before use. CP (2.5 wt % acetyl, 45 wt % propionyl content, $M_n = 7.5 \times 10^4$) was used as purchased from Aldrich Chemical Co.

Preparation of Blends and Uniaxial Drawing. The blends of PHB and CP with different weight ratios, 9/1, 7/3, 5/5, and 3/7 (PHB/CP, w/w), were obtained by a solvent-casting method using chloroform as a cosolvent. Since PHB samples with high crystallinity (especially UHMW-PHB) did not dissolve completely in chloroform at room temperature, all of the homogeneous solutions were prepared in a high-pressure bottle at 100 °C, at which the mechanical mixing was performed for the shortest possible time of about 15 min to avoid the thermal degradation of PHB. After being cooled to room temperature, the blend solutions were subsequently poured into glass Petri dishes, and kept at room temperature for 48 h to allow gradual evaporation of the solvent. The resultant films were dried once again under vacuum for at least 48 h to thoroughly remove the solvent.

The glass transition temperature for common miscible blends is well-known to be strongly dependent on the blend ratio. However, although PHB/CP blends are miscible over the whole composition range, their glass transition temperatures detected by DSC measurement were independent of their composition at the low cellulose ester content, and quite broad or not detected at the high cellulose ester content, which made it difficult to determine drawing temperatures for respective samples. For this reason, a preliminary drawing test for fixing on the drawing temperature was carried out at various temperatures with reference to the previous report[1] in which the T_g values were obtained by dynamic mechanical measurements. The drawing temperatures for respective compositions and the feasible maximum draw ratio at that temperature are listed in Table 1. Although the blend with higher CP content should be stretched at higher temperature, the feasible maximum draw ratio decreased with increasing CP content due to the stiff chain nature and high friction coefficient of the CP component, causing a restraint of chain slippage and necking.

The samples for drawing were cut into 3 cm × 1 cm strips, hot-pressed between two Teflon sheets at 200 °C, and then rapidly quenched in ice−water to preserve the state of amorphous preform, where the sample thickness was controlled to 0.05 mm. The melt-quenched strip was gripped to a portable drawing device designed for stretching up to a maximum of 30 times by hand-operation. The initial gauge length and draw rate were 10 mm and approximately 50 mm/min, respectively. In the case of the PHB-rich blends containing 0−30 wt % CP, the drawing procedure was carried out simultaneously with quenching in water medium. The actual temperature of the water medium was controlled to the desired temperature by adding bits of ice. On the other hand, the samples with a higher CP content of 50−100 wt % were immediately placed into a heating oven adjusted to the given drawing temperature after gripping to the drawing device, subsequently kept for 1 min to be thermally stabilized, and then stretched to a given draw ratio. All of the drawn samples were thermally annealed under tension in a heating oven at 100 °C for 3 h and aged for more than 3 days at room temperature.

Characterization. Thermal characteristics of the blends were measured using a Perkin-Elmer DSC Pyris 1. Sealed aluminum sample pans containing 4−6 mg of materials were employed in all experiments. At the beginning of each experiment, the sample was heated to 200 °C, maintained for 3 min to eliminate its thermal history, and then rapidly cooled to −70 °C. The actual measurement was recorded during the second heating from −70 to +200 °C at a heating rate of 10 °C/min.

To verify how much the crystallization rate of PHB is affected by blending with CP, the isothermal crystallization was also performed at 100 °C, at which the crystallization rate was comparatively fast for PHB blends as well as for PHB homopolymer.[4] The sample was first melted at 200 °C and rapidly cooled to 100 °C. The heat flow signal was recorded until no change of the signal was detected.

Two-dimensional wide-angle X-ray diffraction (WAXD) and small-angle X-ray scattering (SAXS) images of stretched samples were obtained using an X-ray diffractometer (RINT UltraX 18, Rigaku, Japan) equipped with an imaging plate (BAS-SR 127, Fuji Film Co., Japan). The X-ray source was Ni-filtered Cu Kα radiation (wavelength 0.154 nm) generated at 40 kV and 200 mA and collimated by a pinhole collimator with 0.5 mm diameter. The distance from the sample to the imaging plate was 4 cm for WAXD and 50 cm for SAXS. The samples were mounted with the drawing direction vertical. The exposure time was 30 min for WAXD and 180 min for SAXS. In the case of SAXS images, the background involving air scattering was eliminated for obtaining high contrast, by subtracting the empty beam scattering signals taken without sample at the same conditions.

The changes in birefringence of drawn films before and after annealing were measured by using an optical microscope (Nikon ECLIPSE-E600-POL) equipped with a crossed polarizer and first-order red plate compensator (530 nm retardation). The mechanical property was measured using a tensile testing machine (EZtest, Shimadzu Co., Japan) at a crosshead speed of 20 mm/min.

Results

Thermal Properties and Isothermal Crystallization. Figure 1 shows DSC thermograms of bacterial PHB/CP and UHMW-PHB/CP blends with various compositions. For neat bacterial PHB, a sharp exothermal peak and melting peak are detected at 50 and 165 °C, respectively. Although the glass transition of UHMW-PHB appears at the same temperature of about 0 °C as that of the bacterial one, the melting point (177 °C) and heat of fusion ($\Delta H_f = 50.5$ J/g) of UHMW-PHB are considerably higher than those of bacterial PHB ($T_m = 165$ °C, $\Delta H_f = 38.4$ J/g), which is strongly connected with enhanced crystal perfection caused by ultrahigh molecular weight. In general, a longer chain length lowers the number of the chain ends acting as a defect within crystals. In the case of neat CP, only a broad glass transition, as expected for totally amorphous polymer, is observed around 100−150 °C.

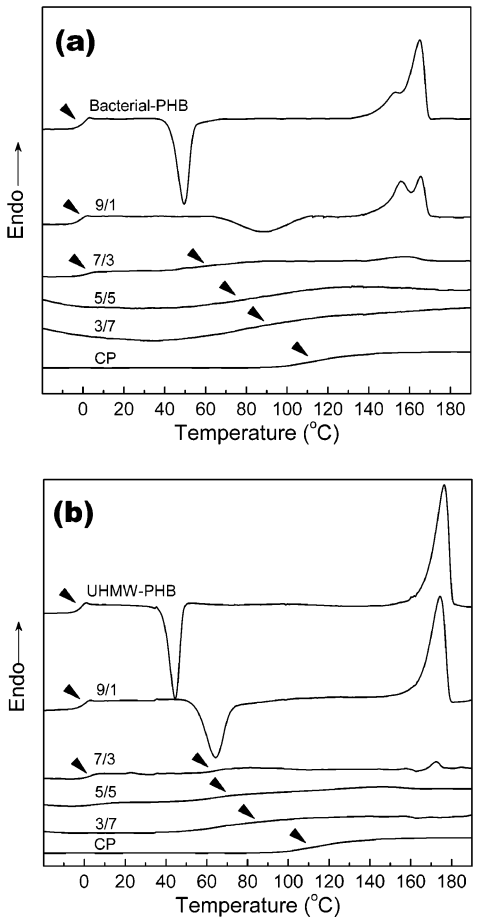

Figure 1. DSC thermograms of (a) bacterial PHB/CP and (b) UHMW-PHB/CP blends obtained from the second heating run with a heating speed of 10 °C/min. The arrows indicate glass transition regions.

Two blend systems show almost the same thermal behavior regardless of the PHB identity. The glass transition temperature (T_g) of the blends is not composition-dependent in the whole composition range, which is in accordance with the previous results.[1−5] For the blend containing 10 wt % CP, the T_g is slightly higher than neat PHB's T_g. However, at 30 wt % CP content, another broad glass transition, except for the low-temperature transition at about 4 °C, is observed around 50−80 °C. When the amount of CP is 50 wt % or more, the low-temperature transition disappears, but the high-temperature transition becomes quite broad and shifted in position to higher temperature with increasing CP content. At first glance, such a trend can be taken as evidence for an immiscible or a partially miscible system. However, Scandola et al.[1−3] have convincingly argued that these systems are, in fact, fully miscible over the entire composition range, and interpreted that the broad and dual transitions are attributed to two mobilization processes in a homogeneous mixture rather than to morphological heterogeneity. Buchanan et al.[7] have also verified the two mobilization processes in the homogeneous melt by means of ^{13}C NMR analysis and suggested that the origin is the different chemical structures of the two components; that is, flexible PHB chains are generally random coils with good molecular mobility, while cellulose esters are rigid extended helices or ribbons in the amorphous phase. Finally, they have concluded that the dual transitions result not from nonequivalent free volumes but rather from nonequivalent molecular motions of components with equivalent free volumes.

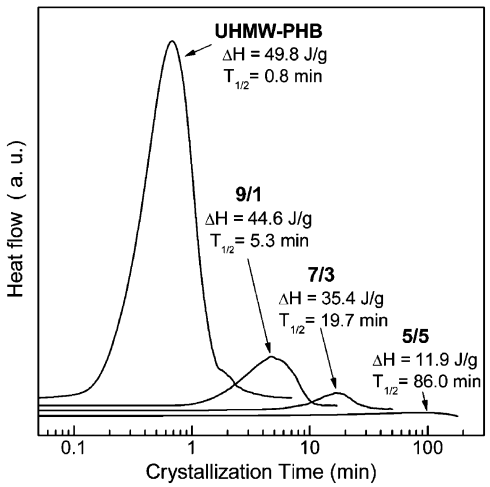

Figure 2. DSC exotherms of UHMW-PHB/CP blends during isothermal crystallization at 100 °C. $T_{1/2}$ indicates the half-life time of the crystallization.

The crystallization behavior was found to be significantly affected by addition of the CP component. As can be seen in Figure 1, the cold-crystallization peak becomes broader and markedly shifts in position to higher temperature even at 10 wt % CP, and the enthalpy is also considerably reduced with increasing CP content, which suggests a significant retardation of crystallization of PHB even at a small amount of CP. This could be explained by not only favorable interaction between two components at the crystal surface but also hindered chain mobility by the rigid CP chains. When the CP content exceeds 30 wt %, neither the melting peak nor the cold-crystallization peak is detected.

To evaluate how much the crystallization rate is affected by blending with cellulose propionate, the isothermal crystallization was performed at 100 °C and is presented in Figure 2. As expected, the isothermal crystallization is also significantly retarded with increasing CP content. Although the apparent crystallization enthalpy decreased inversely proportional to the CP content, the value after correction with the weight fraction of the PHB component remained roughly constant at about 50 J/g in the region 0−30 wt % CP, which is in good agreement with the previous report about PHB/CAB blends that the attainable crystallinity of PHB was only slightly influenced by the blend composition because the PHB chains must be disentangled from the CAB segments as crystallization proceeds.[6] However, further addition of CP brings about a rapid decrease in crystallinity, and eventually, no crystallization trace was detected even for a quite long-term examination as the CP content exceeded 50 wt %.

WAXD Analysis. WAXD photographs of the drawn PHB/CP blend films are displayed in Figure 3. Pure PHB and PHB/CP 9/1 blends exhibit the well-defined oriented patterns of the PHB α-crystal having an orthorhombic lattice structure of $a = 0.576$ nm, $b = 1.320$ nm, and $c = 0.596$ nm with its chain conformation in the left-handed 2/1 helix, which is identified in previous reports.[12−14] The crystalline orientation direction follows an ordinary c-axis orientation, indicating that the main reflections of the (020) and (110) planes ($2\theta = 13.2°$ and 17.2°, respectively) are concentrated on the equator and the (002) reflection lies on the meridian,

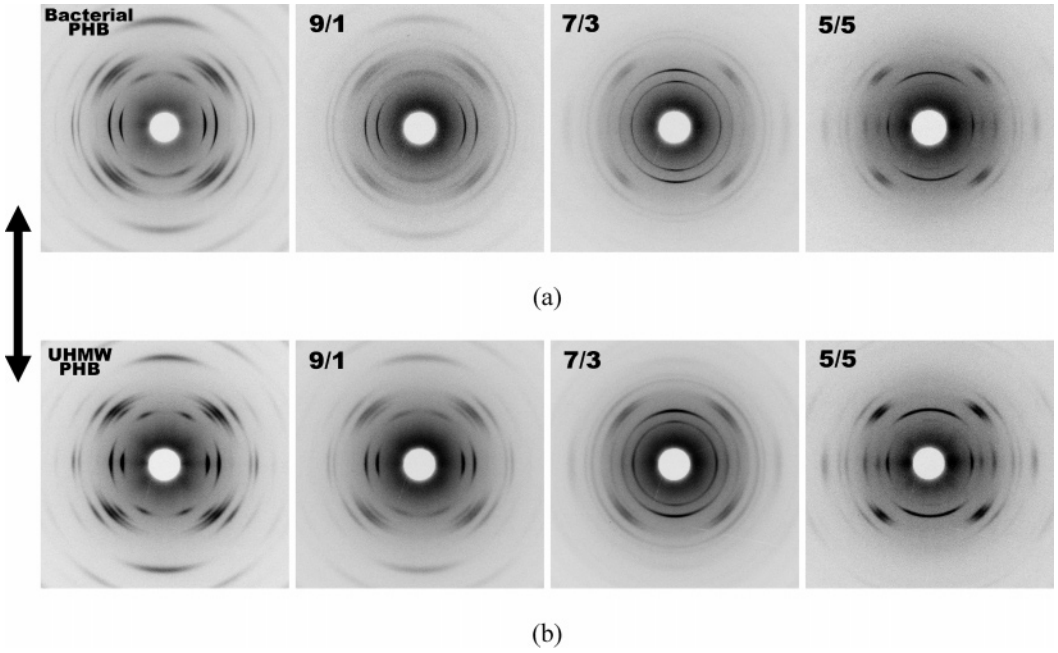

Figure 3. WAXD photographs of (a) bacterial PHB/CP and (b) UHMW-PHB/CP blends drawn to $\lambda = 5$ and annealed at 100 °C for 3 h. The arrow indicates the drawing direction.

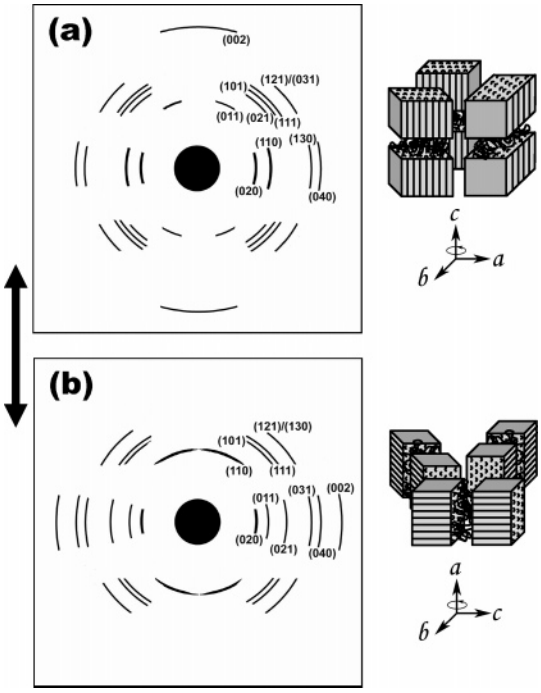

Figure 4. Schematic diagrams of WAXD patterns for (a) the *c*-axis-oriented and (b) the *a*-axis-oriented crystal in PHB/CP blends, which was predicted by using the Cerius[2] software (Accelrys, Inc.) with atomic coordinates reported by Yokouchi et al.[14] On the right side, probable arrangements of PHB lamellae based on corresponding WAXD patterns are schematically illustrated.

which has been verified by comparison with a schematic diagram of the diffraction pattern of the *c*-axis-oriented crystal predicted by using the Cerius[2] software (Accelrys, Inc.) with atomic coordinates reported by Yokouchi et al.[14] (Figure 4a). Since the fiber axis for PHB is the *c*-axis,[13] the molecular chains in the crystal are oriented parallel to the stretching direction. However, when the CP content is 30 wt % or higher, the diffraction pattern is no longer the *c*-axis orientation. The (110) reflection lies on the meridian, and the position of the (020) reflection is also changed dependent on the blend composition. Particularly for the drawn 5/5 blend in Figure 3, the diffraction pattern is exactly identical to a schematic diagram for the *a*-axis orientation as illustrated in Figure 4b, where the crystallographic *a*-axis is arranged preferentially along the stretching direction but the *b*- and *c*-axes are in a plane perpendicular to the stretching direction. Such an orientation behavior is the same regardless of the type of the PHB component. The UHMW-PHB system merely provides more intense and higher oriented textures, indicating higher crystallinity and higher degree of orientation, respectively. For this reason, the UHMW-PHB/CP blend system was employed for further detailed study to verify the origin of such an uncommon orientation.

Figure 5 presents the intensity profiles along the azimuthal angle of the (020) and (110) reflections of UHMW-PHB/CP blends with different draw ratios. The drawn PHB/CP 9/1 blend shows the same orientation as pure PHB regardless of the draw ratio. However, the reflection peaks along the azimuthal angle become exceedingly broad, which indicates a significant decrease in the degree of orientation. For the 7/3 blend at a draw ratio (λ) of 3, the two (020) reflections are located at azimuthal angles of 0° and 180°, whereas the (110) reflection appears quite broadly with the center at ±90°, which corresponds to the *b*-axis being aligned preferentially along the stretching direction. At a higher draw ratio ($\lambda = 5$), the additional broad (020) reflections are detected at azimuthal angles of ±90°, and besides, the positions of the (110) reflection shift to 0° and 180°, which corresponds to the *a*-axis orientation. From these results, it is found that the drawn 7/3 blend has two types of crystals with different crystalline orientations, the *a*-axis and *b*-axis orientations, and among them, the amount of the *a*-axis-oriented crystal tends to increase preferentially with the draw ratio. On the contrary, the 5/5 blend has only the *a*-axis orientation, indicating the (020) reflections at azimuthal angles of ±90° and the (110) reflections near 0° and 180°. At a higher draw ratio, the (020) reflections become narrower, and fur-

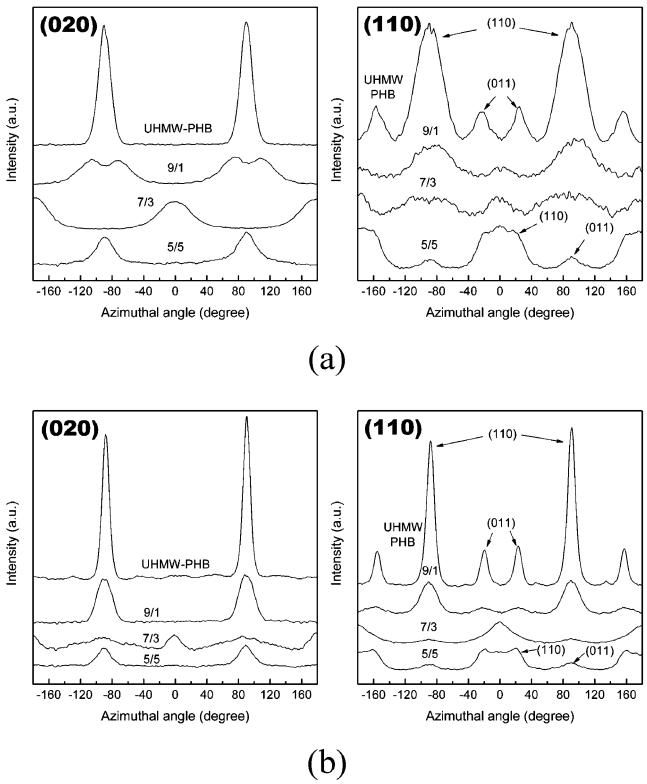

Figure 5. Azimuthal profiles of (020) and (110) reflections obtained from WAXD patterns of UHMW-PHB/CP blends at (a) $\lambda = 3$ and (b) $\lambda = 5$ and annealed at 100 °C for 3 h. The drawing direction corresponds to an azimuthal angle of 0°.

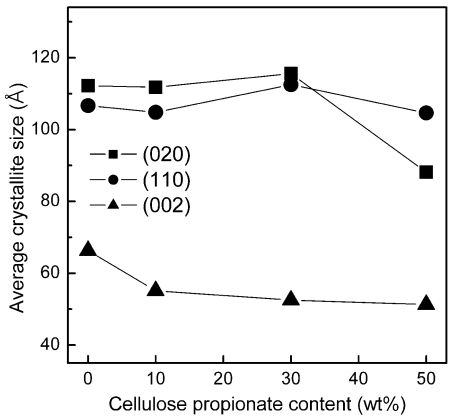

Figure 6. Average crystallite size as a function of CP content for drawn UHMW-PHB/CP blends ($\lambda = 5$).

ther, the (110) reflection near 0° splits clearly into a double peak at ±21°, which is roughly close to the ideal value of ±23.7° from calculation when the crystallographic *a*-axis of the PHB crystal is perfectly parallel to the stretching direction. From these WAXD results, it has been concluded that the crystallization manner of the PHB component under strain changes from *c*-axis-oriented growth to *a*-axis-oriented growth with increasing CP content, and that this tendency is more predominant at a higher draw ratio.

The average sizes of the PHB crystallites were obtained from the integral breadth of the reflections by using the Scherrer equation,[15] and the result is plotted in Figure 6. In the 0−30 wt % CP content range, the crystallite sizes obtained from the (002) reflection decrease with increasing CP content, but those from the (020) and (110) reflections increase slightly, a tendency which is similar to the result of undrawn blends by Buchanan et al.[7] However, at 50 wt % CP content, all the crystallite sizes became smaller. Particularly, the value of the (020) reflection diminishes more markedly and consequently becomes smaller than that of the (110) reflection. Considering that the size obtained from the (110) reflection involves information along the *a*-axis as well as along the *b*-axis, this reversion of the sizes can be strongly connected with the change of crystallization manner toward the *a*-axis-oriented crystal growth, which will be discussed again with the crystal growth mechanism in the Discussion.

Effect of the Annealing Temperature. To investigate the effect of the annealing temperature on the orthogonal orientation, the drawn samples were annealed at various temperatures and their crystalline orientations were examined. WAXD photographs of UHMW-PHB/CP 7/3 and 5/5 blends ($\lambda = 5$) annealed at various temperatures and the azimuthal profiles of the main reflections are shown in Figures 7 and 8. In the case of the 7/3 blend, the overall diffraction patterns become more intense and the widths of (110) reflections at azimuthal angles of 0° and 180° become narrower with increasing annealing temperature (Figure 8a). For the (020) reflection, four peaks are observed at 0°, ±90°, and 180°. At higher temperature, the peaks at ±90° become stronger, while the peaks at 0° and 180° become weaker. This demonstrates that the *b*-axis of the PHB crystal is aligned more preferentially perpendicular to the drawing direction at higher annealing temperature. In other words, the amount of the *a*-axis-oriented crystal increases preferentially in proportion to the annealing temperature.

In the case of the 5/5 blend, the PHB component did not crystallize at temperatures lower than 80 °C. In the temperature region of 100−120 °C, the width of the (020) reflection is the narrowest, and further, the (110) reflection near 0° clearly splits into a double peak located at ±21°, indicating that the degree of *a*-axis orientation is the highest in this temperature region. At even higher temperature (140 °C), the (020) reflection becomes diffused and the (110) reflection also returns to a single peak, suggesting that the degree of *a*-axis orientation is rather reduced at this temperature.

SAXS Analysis. The orthogonal crystalline orientation depending on the composition was also clearly revealed in the SAXS patterns. Figure 9 shows SAXS patterns of pure UHMW-PHB and its blends with CP after stretching to $\lambda = 5$ and annealing at 100 °C for 3 h. Pure PHB and the PHB/CP 9/1 blend show well-defined meridional (vertical) spots, indicating that the lamellae are stacked along the drawing direction. At a higher CP content, 30−50 wt %, the dominant feature is the equatorial (horizontal) streaks instead of meridional spots, meaning that a periodic structure is perpendicular to the stretching direction. The periodic lengths were determined from the maxima of scattering intensities from meridional scans for PHB and the 9/1 blend, and from equatorial scans for the 7/3 and 5/5 blends by using Bragg's equation ($L = \lambda/(2 \sin \theta)$). Generally, in a crystalline/amorphous blend system, the change of the long period can be an indicator to judge the segregation of the amorphous component. According to a previous study on undrawn PHB/CE blends,[6] most amorphous CE units were segregated in the interlamellar region due to the low diffusivity of the CE molecules, which reflected the increase in a long spacing of the PHB

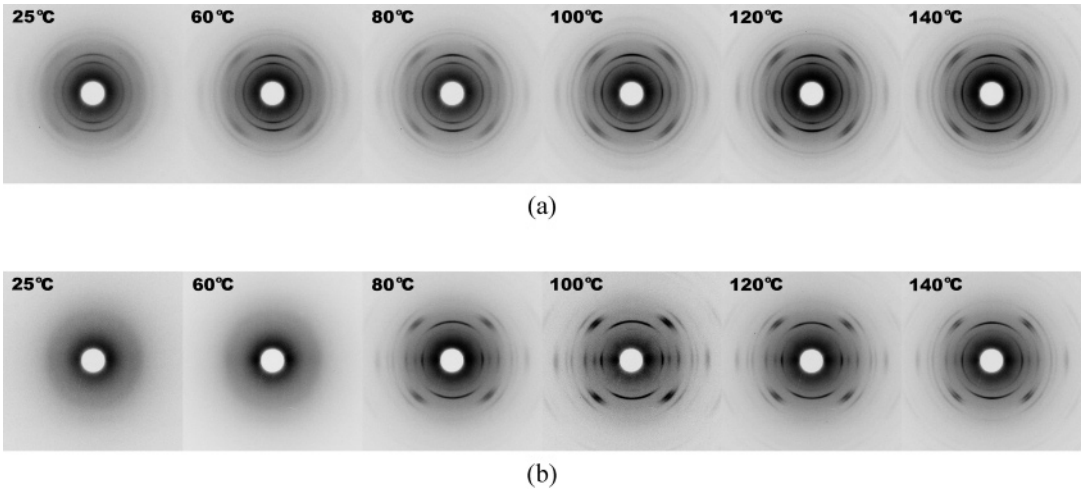

Figure 7. WAXD photographs of UHMW-PHB/CP (a) 7/3 and (b) 5/5 blends ($\lambda = 5$) annealed at various temperatures for 3 h.

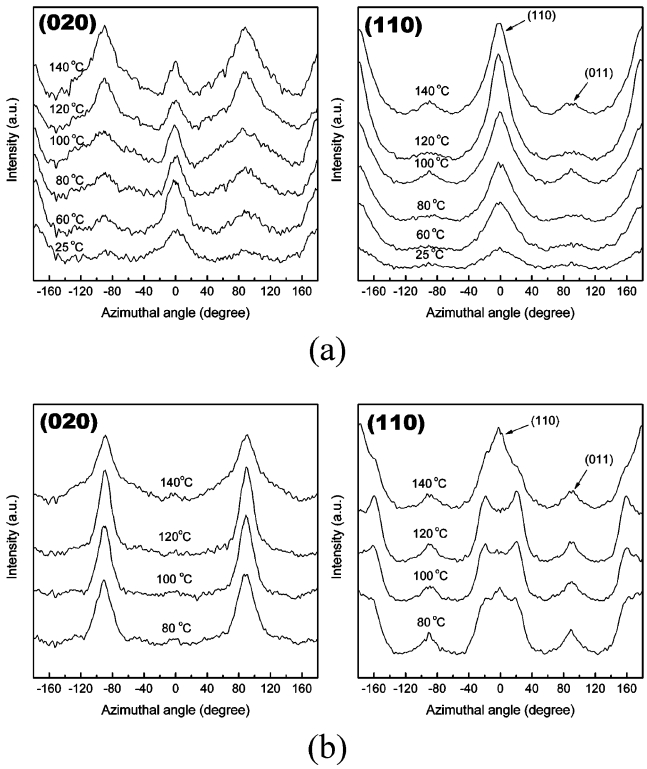

Figure 8. Azimuthal profiles of (020) and (110) reflections obtained from WAXD patterns of UHMW-PHB/CP (a) 7/3 and (b) 5/5 blends ($\lambda = 5$) annealed at various temperatures for 3 h.

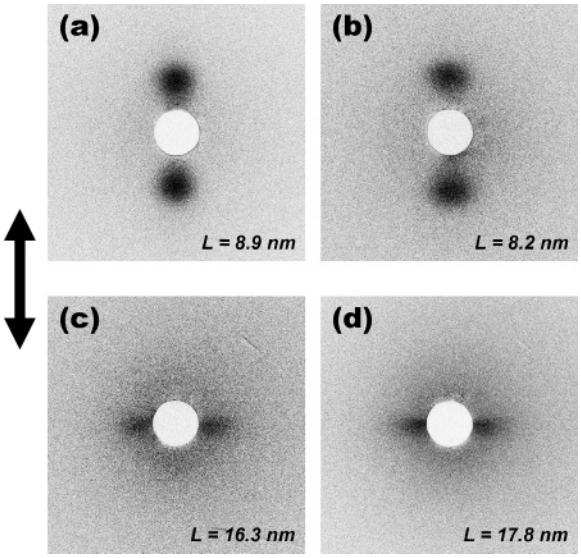

Figure 9. SAXS patterns of (a) pure UHMW-PHB and UHMW-PHB/CP blends, (b) 9/1, (c) 7/3, and (d) 5/5, after drawing to $\lambda = 5$ and annealing at 100 °C for 3 h. The arrow represents the drawing direction.

lamellar stacks. However, in the present case, the addition of 10 wt % CP results in a slight decrease in the long period from 8.9 to 8.2 nm, indicating that the CP molecules were not situated within PHB lamellar stacks but segregated out of interlamellar zones. On the other hand, the drawn blends containing 30−50 wt % CP reveal that the periodic length (16−18 nm) perpendicular to the stretching direction is much higher than the long period of pure PHB. These results can be regarded as good information for estimating the location of the extended CP molecules, which will be discussed in the Discussion.

Birefringence. It is of interest to measure the birefringence of the stretched blends, particularly the samples with orthogonal chain orientation, because the birefringences of two components are contrary to each other. The PHB molecules are widely known to be negatively birefringent;[12] i.e., the refractive index in the chain direction is smaller than in the perpendicular direction. On the contrary, the CP molecules are positively birefringent. The birefringence signs of the drawn samples before and after annealing could be simply determined by using a first-order red plate (530 nm retardation) in a polarized optical microscope (POM).

As expected, the drawn PHB had a negative value, while the drawn CP and PHB/CP 3/7 blend showed a positive birefringence regardless of annealing. For the drawn 7/3 blend, fast relaxation and crystallization during POM observation at room temperature made it impossible to measure the birefringence in a completely amorphous state. We could only find that the birefringence after annealing was positive. However, the drawn 5/5 blend did not crystallize and maintained its amorphous state at room temperature, which allows the birefringence before and after annealing to be measured. The drawn sample before annealing showed only negligible birefringent light, which indicates almost nonbirefringence. For this reason, we could not supply a micrograph before annealing under a crossed polarizer. Instead, the micrograph taken without a crossed polar-

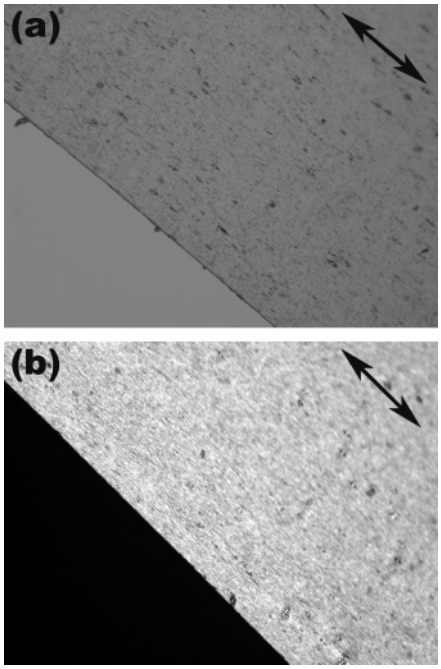

Figure 10. Optical micrographs of the UHMW-PHB 5/5 blend drawn to $\lambda = 5$ (a) before annealing and (b) after annealing at 100 °C for 3 h. The micrographs were taken with 50× magnifications at room temperature. The arrow indicates the drawing direction. Micrograph (a) was taken without a crossed polarizer, because we could not obtain a micrograph with good contrast under the crossed polarizer due to the negligible birefringent light. On the contrary, micrograph (b) could be taken with an insertion of the crossed polarizer.

izer is presented in Figure 10a. This nonbirefringence does not mean nonorientation of the two components, but rather results from the contrary birefringence signs between the PHB and CP components although both the amorphous chains are oriented parallel to the drawing direction. On the other hand, for the drawn sample after annealing, the strong positive birefringence light was observed as shown in Figure 10b, which is obvious evidence to prove an orthogonal alignment of PHB molecules in the crystal.

Discussion

Crystal Growth Model. An occurrence of orthogonal orientation has been reported occasionally in heterogeneous systems such as block copolymers, immiscible blends, and organic/inorganic composites. To interpret such a behavior, several models involving the epitaxial crystallization,[16−18] thermal shrinkage stress,[19,20] confinement of crystal growth,[21−29] and trans crystallization[30,31] have been employed. However, it has been a rare occurrence for homogeneous systems. Recently, Zhao and co-workers have reported a unique finding in the orientation behavior of miscible poly(ϵ-caprolactone)/poly(vinyl chloride) blends[32] which is very similar to the present result and interpreted that finding with the intramolecular nucleation model. Crystallization under strain generally leads to a segmental chain orientation parallel to the strain direction, which originates from linear nuclei produced by a row nucleation of extended molecular chains as schematically illustrated in Figure 11a. In this case, the essential conditions are a rapid crystallization and high enough draw ratio to form row nucleation. On the other hand, the perpendicular crystalline orientation is the result of the intramolecular nucleation (Figure 11b): First, there is chain relaxation

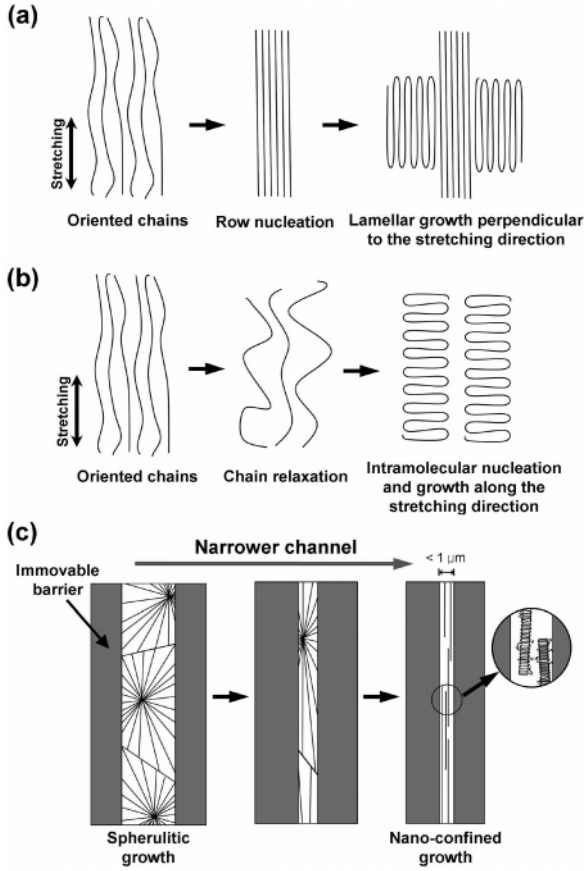

Figure 11. Schematic illustration of two nucleation mechanisms of extended molecular chains, (a) row nucleation with parallel crystalline chain orientation and (b) intramolecular nucleation with perpendicular crystalline chain orientation, and of (c) the nanoconfined crystal growth model.

prior to nucleation involving longitudinal chain retraction and necessarily some kind of chain folding, which could be allowed for miscible systems having a reduced crystallization rate induced by a favorable interaction with the second component. The resultant chain-folding can initiate the intramolecular nucleation (folded chain nucleation), and as a result, the lamellae with chain orientation perpendicular to the drawing direction are produced as shown in Figure 11b.

This hypothesis seems to be quite persuasive and also available for interpreting the present results. However, there is no consideration for a role of the second component except lowering the crystallization rate. Our belief is that the extended second component having a stiff nature can geometrically affect the crystallization behavior of the flexible component under strain. Especially in PHB/CP blends, the CP chains could be expected to have a ribbonlike shape and motion in the blends similarly to other cellulose derivatives due to the anisotropic cellobiose unit with a wide difference in chain dimension between the wide axis (>1 nm) and narrow axis (0.4−0.5 nm),[33] which increases the probability that the highly extended CP chains can affect the crystallization and orientation behavior of PHB. In this respect, the nanoconfined crystal growth among several models could be employed as another mechanism to explain the geometrical effect of extended CP molecules. The confined crystallization has been reported to occur in narrow channels formed by inorganic fibers,[21] a drawn polymer matrix,[22−24] an ordered block copolymer,[25−28] and cylindrical morphologies.[29] Gener-

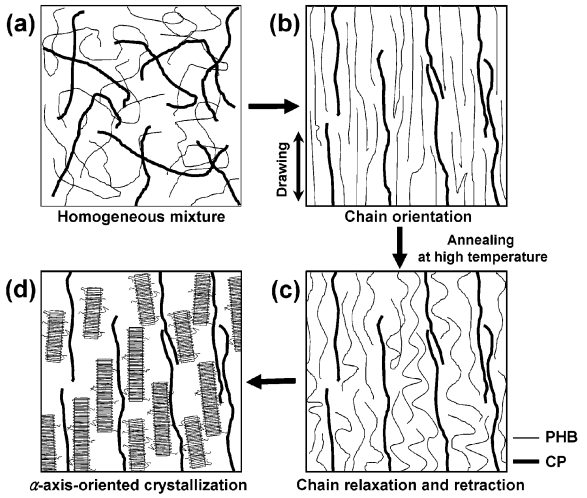

Figure 12. Schematic illustration of drawing and crystallization behavior of PHB/CP blends containing 30−50 wt % CP.

ally the crystallization manner of most semicrystalline polymers in sufficient isotropic space is a spherulitic growth that lamellar bundles grow up radially from a nucleus. In contrast, when the highly anisotropic gap is formed by some fences and the width of the short axis is narrower than the distance between neighboring crystal nuclei, the result is a highly anisotropic growth as shown in Figure 11c although the growth around the nuclei proceeds radially in the same manner as in spherulite. If the width of the short axis is quite narrow, in the nanometer range, it does not matter if the crystal growth proceeds along the long axis of the narrow channel, because the growths toward other directions are negligible, in which the axis of fastest crystal growth is aligned preferentially along the long axis of the narrow gap and other axes lie in a plane perpendicular to the long axis. Recently, Li et al.[24] have suggested that the perpendicular crystalline orientation of poly(butylene succinate) (PBSU) in a miscible blend with poly(vinylidene fluoride) (PVFD) was induced by confined crystallization in the nanosized domains. However, this system differs from our case in the origin of the narrow gap. In that case, the crystal domains of the earlier crystallized PVDF phase played a role as a barrier for forming the narrow gap.

Drawing and Crystallization Behavior of PHB/CP Blends. To interpret the unique orientation and crystallization behavior in PHB/CP blends, we have suggested a mechanism based on intramolecular nucleation and confined crystal growth as schematically represented in Figure 12.

In the first step (Figure 12a), the amorphous preform before the drawing procedure is a homogeneous mixture of two components, which has been supported by several efforts.[1−7] In this state, the PHB molecular chains are in random coils, while the CP chains could be expected to be stiff helices or ribbons originated by anisotropic cellobiose units consisting of rigid pyranose rings as noted previously. Such a high stiffness can give rise to less folding and entangling between not only similar chains but also dissimilar chains. The work on PHB/CAB blends by El-shafee et al.[6] revealed that the CAB component did not inhibit the level of crystallinity attained by the PHB component. This means that there is no impediment for disentangement of PHB chains from the cellulose ester segments, which seems to be strongly related to less entanglement between two molecular chains. In the present study, the isothermal crystallization experiment also demonstrated the same result that the corrected enthalpy of crystallization of the PHB component remained roughly constant in the region of 0−30 wt % CP content.

When the homogeneous mixture of PHB and CP is stretched uniaxially, there is no doubt that both the components are oriented along the drawing direction (Figure 12b). In the birefringence result, the drawn 5/5 blend before annealing was found to be almost nonbirefringent. Considering that the birefreingent signs of PHB and CP molecules are contrary to each other, this result could prove the co-orientation of the two components. In this step, it is also probable to assume that the ribbon-shaped CP chains are fully extended and aligned orderly at regular intervals by uniaxial drawing. Under this assumption, the extended CP chains having an anisotropic shape can play a role as a barrier blocking the migration of the PHB molecular chains. In other words, the PHB molecules are confined in quite narrow regions surrounded by the extended CP chains. In addition, the confined PHB component could be expected to be still in the amorphous state due to the low drawing temperature (around T_g) and reduced crystallization rate caused by a favorable interaction with the CP molecules.

The crystallization of PHB occurs during annealing at higher temperature. However, it is hard to expect the *a*-axis-oriented crystal growth with perpendicular chain orientation in the state in which PHB molecular chains are still oriented along the drawing direction. Accordingly, another hypothesis is required as follows: the oriented PHB chains may undergo some relaxation or shrinkage prior to crystallization during annealing at this temperature, whereas the stiff CP chains are not affected and still highly oriented (Figure 12c). Such a selective relaxation of the flexible component at temperatures above the T_g of one component and below that of the other component is no longer extraordinary even for a miscible system, which has been revealed in several works[32,34,35] In the study by Zhao et al.,[32] when the drawn PCL/PVC (50/50) blend was annealed for 20 h where PCL was still amorphous, the PVC component remained highly oriented but the flexible PCL molecules were almost relaxed to an unoriented state.

In the final step, the relaxed PHB molecules with chain folding can form intramolecular nuclei with chain orientation perpendicular to the drawing direction in the same manner as described previously in Figure 11b. Consequently, the crystal growth proceeds slowly along the long axis of the narrow gap between the extended CP chains as schematically illustrated in Figure 12d. Birley et al.[36] have reported the result that the direction of chain folding of PHB, which is identical to the crystallographic *a*-axis, is parallel to the crystal growth differently from common cases, which decisively supports this growth model from intramolecular nucleation.

In the present study, it was found that the factors determining the crystal growth mode of PHB in PHB/CP blends were not only the composition but also the annealing temperature. The higher CP content could result in narrower gaps and slower crystallization, which is the origin of a higher degree of orthogonal crystalline orientation. However, when the CP content exceeded 50 wt %, no trace for crystallization was

detected, indicating that the gaps might become too narrow to crystallize within them.

The *a*-axis orientation was revealed to be more predominant at higher annealing temperature up to 120 °C (Figure 8). This observation appears to be strongly connected with the selective relaxation and retention occurring at temperatures between the T_g values of the two components. The oriented PHB chains can be relaxed more rapidly and preferentially at higher temperature up to 120 °C, which can give rise to the higher degree of *a*-axis orientation. However, an even higher temperature (140 °C) may permit the relaxation of the stiff CP chains acting as a barrier, which are accompanied by probable changes of the narrow gap in width and orientation. Such disordering of the narrow gap can directly affect the orientation of the PHB component. This is responsible for the lowered degree of *a*-axis orientation of PHB at 140 °C in Figure 8. The changes of crystallite sizes with composition in Figure 6 can also be interpreted in terms of the crystal growth mechanism. The crystal growth along the crystallographic *a*-axis inevitably produces crystallites with larger size along the *a*-axis than along other axes, which can explain the result that, for 5/5 blends with the highest degree of *a*-axis orientation, the crystallite size obtained from the (110) reflection including information on the *a*-axis direction became larger than that from the (002) reflection.

In SAXS analysis, the presence of 10 wt % CP resulted in a lower long period than that of pure PHB. This means that the extended CP chains were not located within PHB lamellar stacks but segregated out of lamellar bundles, which is contrary to the previous result for the undrawn case.[6] This can also prove the fact that the CP chains were still extended and oriented along the stretching direction during crystallization of the PHB component. The interlamellar segregation of the extended CP chains is geometrically unrealizable without any changes of their orientation or chain relaxation considering that the CP chain orientation and lamellar stacking are in the same direction. In contrast, the long periodicity to the equatorial direction for 30−50 wt % CP containing blends was significantly higher than that for pure PHB. The scattering on the equator was attributed to the difference in electron density between the *a*-axis-oriented PHB crystals and aligned amorphous chains involving the extended CP and the uncrystallized PHB molecules as illustrated in Figure 12d. In other words, it can be regarded that the extended CP chains lie in the interlamellar region of the *a*-axis-oriented PHB crystal, which can explain the increase of the long period at higher CP content.

Finally, we studied the effect of the orthogonal chain orientation on the mechanical properties of the blends, particularly in terms of two directions, parallel and perpendicular to the drawing direction. For undrawn blends, it has already been reported that the ductility was greatly enhanced due to the remarked decrease in crystallinity by blending with amorphous CP.[4] However, for the drawn blends of the present study, the tensile strength and modulus toward the parallel direction increased considerably in proportion to the CP content in the draw ratio range of 3−5, whereas the elongation decreased with increasing CP content. Although the 5/5 blend at $\lambda = 5$ had low overall crystallinity and a different chain orientation compared to pure PHB, the tensile strength reached a considerably high value of 124 MPa compared to 45 MPa for pure PHB at the same draw ratio. This stiffening is attributed to the molecular orientation of the CP chains with a rigid nature.

It is very interesting to investigate the mechanical property toward the perpendicular direction of the sample with an orthogonal crystalline chain orientation. However, contrary to our expectation, the stretched samples were too weak toward this direction to determine their values regardless of the blend composition. Even the 5/5 blend with the highest level of perpendicular crystalline chain orientation was easily broken before the yield point. This seems to be due to a lack of tie molecules between the *a*-axis-oriented lamellae caused by the confining effect of the extended ribbon-shaped CP chains as schematically illustrated in Figure 12.

Conclusions

Orientation and crystallization behaviors of PHB in miscible blends with CP were investigated under uniaxial drawing. The results from the X-ray analysis and birefringence observation revealed that the crystalline chain orientation of the PHB component in the blends was either parallel or perpendicular to the stretching direction, which was strongly dependent on the blend ratio, drawing ratio, and annealing temperature. When the CP content was 30−50 wt %, the predominant crystal growth manner was changed from *c*-axis-oriented to *a*-axis-oriented growth where the crystallographic *a*-axis is arranged preferentially along the stretching direction, while the *b*- and *c*-axes are in a plane perpendicular to the stretching direction. In this paper, we suggested a mechanism based on intramolecular nucleation and confined crystal growth to interpret the *a*-axis-oriented crystal growth. First, the fast relaxation of the PHB component in the beginning of the annealing process allows the PHB chains to form the intramolecular nuclei with chain orientation perpendicular to the drawing direction. The crystal growth from these intramolecular nuclei proceeds along the long axis of narrow gaps formed by the extended ribbon-shaped CP chains. As a consequence, the crystal lamellae with chain orientation perpendicular to the stretching direction are produced.

Acknowledgment. This work has been supported by a Grant-in-Aid for Young Scientists (A) from the Ministry of Education, Culture, Sports, Science and Technology (MEXT) of Japan (15685009) and by a SORST (Solution Oriented Research for Science and Technology) grant from the Japan Science and Technology Corp. (JST).

References and Notes

(1) Scandola, M.; Ceccorulli, G.; Pizzoli, M. *Macromolecules* **1992**, *25*, 6441.
(2) Ceccorulli, G.; Pizzoli, M.; Scandola, M. *Macromolecules* **1993**, *26*, 6722.
(3) Pizzoli, M.; Scandola, M.; Ceccorulli, G. *Macromolecules* **1994**, *27*, 4755.
(4) Maekawa, M.; Pearce, R.; Marchessault, R. H.; Manley, R. S. J. *Polymer* **1999**, *40*, 1501.
(5) Wang, T.; Cheng, G.; Ma, S.; Cai, Z.; Zhang, L. *J. Appl. Polym. Sci.* **2003**, *89*, 2116.
(6) El-Shaffee, E.; Saad, G. R.; Fahmy, S. M. *Eur. Polym. J.* **2001**, *37*, 2091.
(7) Buchanan, C. M.; Gedon, S. C.; White, A. W.; Wood, M. D. *Macromolecules* **1992**, *25*, 7373.
(8) Iwata, T.; Tsunoda, K.; Aoyagi, Y.; Kusaka, S.; Yonezawa, N.; Doi, Y. *Polym. Degrad. Stab.* **2003**, *79*, 217.

(9) Aoyagi, Y.; Doi, Y.; Iwata, T. *Polym. Degrad. Stab.* **2003**, *79*, 209.
(10) Iwata, T.; Aoyagi, Y.; Fujita, M.; Yamane, H.; Doi, Y.; Suzuki, Y.; Takeuchi, A.; Uesugi, K. *Macromol. Rapid Commun.* **2004**, *25*, 1100.
(11) Kusaka, S.; Abe, H.; Lee, S. Y.; Doi, Y. *Appl. Microbiol. Biotechnol*. **1997**, *47*, 140.
(12) Okamura, K.; Marchessaults, R. H. In *Conformation of biopolymers*; Ramachandra G. N., Ed.; Academic Press: New York, 1967; Vol 2, p 709.
(13) Cornibert, J.; Marchessault, R. H. *J. Mol. Biol.* **1972**, *71*, 735.
(14) Yokouchi, M.; Chatani, Y.; Tadokoro, H.; Teranishi, K.; Tani, H. *Polymer* **1973**, *14*, 267.
(15) Scherrer, P. *Gottinger Nachrichten* **1918**, *2*, 98.
(16) Fornes, R. E.; Grady, P. L.; Hersh, S. P.; Bhat, G. R. *J. Polym. Sci., Polym. Phys. Ed.* **1976**, *14*, 559.
(17) Seth, K. K.; Kempster, C. J. E. *J. Polym. Sci., Polym. Symp.* **1977**, *58*, 297.
(18) Wiyatno, W.; Pople, J. A.; Gast, A. P.; Waymouth, R. M.; Fuller, G. G. *Macromolecules* **2002**, *35*, 8498.
(19) Gross, B.; Petermanm, J. *J. Mater. Sci.* **1984**, *19*, 105.
(20) Kojima, M.; Satake, H. *J. Polym. Sci., Polym Phys. Ed.* **1984**, *22*, 285.
(21) Waddon, A. J.; Hill, M. J.; Keller, A.; Blundell, D. J. *J. Mater. Sci.* **1987**, *22*, 1773.
(22) Mencik, Z.; Plummer, H. K.; Oene, H. V. *J. Polym. Sci., Part A-2* **1972**, *10*, 507.
(23) Schultz, J. M. *J. Polym. Sci., Part B: Polym. Phys.* **1992**, *30*, 785.
(24) Li, Y.; Kaito, A.; Horiuchi, S. *Macromolecules* **2004**, *37*, 2119.
(25) Hamley, I. W.; Fairclough, J. P. A.; Terrill, N. J.; Ryan, A. J.; Lipic, P. M.; Bates, F. S.; Towns-Andrews, E. *Macromolecules* **1996**, *29*, 8835.
(26) Zhu, L.; Calhoun, B. H.; Ge, Q.; Quirk, R. P.; Cheng, Z. D.; Thomas, E. L.; Hsiao, B. S.; Yeh, F.; Liu, L.; Lotz, B. *Macromolecules* **2001**, *34*, 1244.
(27) Potemkin, I. I. *Macromolecules* **2004**, *37*, 3505.
(28) Huang, P.; Zhu, L.; Guo, Y.; Ge, Q.; Jing, A. J.; Chen, W. Y.; Quirk, R. P.; Cheng, S. Z. D.; Thomas, E. L.; Lotz, B.; Hsiao, B. S.; Avila-Orta, C. A.; Sics, I. *Macromolecules* **2004**, *37*, 3689.
(29) Huang, P.; Zhu, L.; Cheng, S. Z. D.; Ge, Q.; Quirk, R. P.; Thomas, E. L.; Lotz, B.; Hsiao, B. S.; Liu, L.; Yeh, F. *Macromolecules* **2001**, *34*, 6649.
(30) Li, Y. J.; Kaito, A. *Macromol. Rapid Commun.* **2003**, *24*, 255.
(31) Li, Y. J.; Kaito, A. *Macromol. Rapid Commun.* **2003**, *24*, 603.
(32) Zhao, Y.; Keroack, D.; Prud'homme, R. *Macromolecules* **1999**, *32*, 1218.
(33) Kondo, T.; Togawa, E.; Brown, R. M. *Biomacromolecules* **2001**, *2*, 1324.
(34) Faivre, J. P.; Jasse, B.; Monnerie, L. *Polymer* **1985**, *26*, 879.
(35) Zhao, Y.; Jasse, B.; Monnerie, L. *Polymer* **1989**, *30*, 1643.
(36) Birley, C.; Briddon, J.; Sykes, K. E.; Barker, P. A.; Organ, S. J.; Barham, P. J. *J. Mater. Sci.* **1995**, *30*, 6335.

MA0481611